

CrystEngComm

Accepted Manuscript



This is an *Accepted Manuscript*, which has been through the Royal Society of Chemistry peer review process and has been accepted for publication.

Accepted Manuscripts are published online shortly after acceptance, before technical editing, formatting and proof reading. Using this free service, authors can make their results available to the community, in citable form, before we publish the edited article. We will replace this *Accepted Manuscript* with the edited and formatted *Advance Article* as soon as it is available.

You can find more information about *Accepted Manuscripts* in the [Information for Authors](#).

Please note that technical editing may introduce minor changes to the text and/or graphics, which may alter content. The journal's standard [Terms & Conditions](#) and the [Ethical guidelines](#) still apply. In no event shall the Royal Society of Chemistry be held responsible for any errors or omissions in this *Accepted Manuscript* or any consequences arising from the use of any information it contains.

COMMUNICATION

ROD-8, a rod MOF with pyrene-cored tetracarboxylate linker: framework disorder, derived nets and selective gas adsorption†

Cite this: DOI: 10.1039/x0xx00000x

 Ru-Jin Li,^a Mian Li,^a Xiao-Ping Zhou*,^a Seik Weng Ng,^b Michael O’Keeffe*^c and Dan Li*^a

Received 00th January 2014,

Accepted 00th January 2014

DOI: 10.1039/x0xx00000x

www.rsc.org/crystengcomm

Reported here is a new Cd^{II}-based metal-organic framework (MOF), ROD-8, based on rod secondary building unit (SBU) and tetratopic linker 1,3,6,8-tetrakis(*p*-benzoic acid)pyrene. The structure of this MOF experiences framework disorder with two extreme ordered orientations of the ligand, which are topologically related to two nets, namely lrk and lrl, both derived from the basic net lrl. Moreover, the activated sample, ROD-8a, shows selective gas adsorption of CO₂ over N₂, CO₂ over CH₄ and CH₄ over N₂ at room temperature, estimated by the Ideal Adsorbed Solution Theory (IAST).

In the past decade, metal-organic frameworks (MOFs), which are assembled from metal ions or clusters and organic linkers to form crystals with potential voids,¹ have attracted widespread attention owing to their fascinating structures and topologies,² as well as various applications such as gas storage and separation,³ catalysis,⁴ sensing,⁵ and so on. The incorporation of varied connectors and linkers into coordination networks has resulted in many pleasing and complicated MOF structures. In this regard, the identification and classification of the underlying nets^{2b-d} of MOFs are important for further theoretical and applied studies. Recently, a large number of new MOFs have been reported with more complicated topologies, notably including two main categories: one with 1-periodic metal secondary building units (rod SBUs)^{2b} and the other with polytopic organic linkers.^{2c,6} However, the number of MOFs containing both rod SBUs and polytopic linkers is small, and the best method for deconstructing such type of MOFs into their underlying nets is not entirely clear.

Apart from the interest on structures, because of their high surface areas and tunable pore sizes and surface properties, MOFs are now seriously considered for the applications in gas storage and separation.³ Recent hot topics of MOF applications for clean energy and environmental protection include CO₂ capture and separation^{3c,d} and CH₄ storage.^{3g,h} The rational consideration of selective gas adsorption must take into account

the physical property (e.g. polarizability and quadrupole moment) of the gas molecules and also the host-guest interactions.^{3e,7} For example, the incorporation of large, planar aromatic or methyl-substituted ligands, which then form a pore size suited to the kinetic diameter of methane, can increase the CH₄ uptake capacity of MOFs.^{3a,g} The gas separation selectivity is best evaluated by the Ideal Adsorbed Solution Theory (IAST),^{3d,e,8} rather than merely comparing the uptake capacities.

The authors have been interested in rod MOFs (i.e. MOFs with rod SBUs).^{2b,9} Herein, we report a Cd^{II}-based three dimensional (3D) MOF, [Cd₂(TBAPy)(H₂O)₂·DMF·0.5dioxane (named ROD-8, DMF = dimethylformamide), constructed from a tetratopic linker with a π -conjugated pyrene core, i.e. 1,3,6,8-tetrakis(*p*-benzoic acid)pyrene (H₄TBAPy).^{9d,10} The reaction of H₄TBAPy with Cd(NO₃)₂·4H₂O in DMF/dioxane/H₂O (2:1:1) solvent mixture in a sealed pyrex glass tube at 120 °C for 72 hours produced orange block-like crystals of ROD-8 in high yield (see ESI† for experimental detail).

Single crystal X-ray crystallography‡ revealed that ROD-8 crystallizes in the monoclinic space group *P2₁/c*. The asymmetric unit contains two crystallographically independent Cd^{II} ions, one deprotonated TBAPy ligand and two coordinated H₂O. Cd1 is coordinated with seven carboxylate-O from four TBAPy ligands and adopts a distorted pentagonal bipyramidal geometry, while Cd2 exhibits a distorted octahedron, fulfilled by four carboxylate-O from four TBAPy ligands and two coordinated H₂O (Fig. S1 in ESI†). The two Cd^{II} ions are mono- or triply-bridged by the carboxylate groups to generate an infinite 1D metal chain that we call the rod SBU (Fig. 1b). Each tetracarboxylate ligand with eight O donors is linked to eight Cd^{II} ions (Fig. 1a) from four rod SBUs, extending them into a 3D MOF with two types of 1D porous channels (one with window of *ca.* 6.5 × 11.8 Å²; the other *ca.* 8.5 × 9.5 Å²). The direction of the channels accords with that of the rod SBUs (along the *a* axis), and the distance between two nearest parallel pyrene core plane is 4.35 Å.

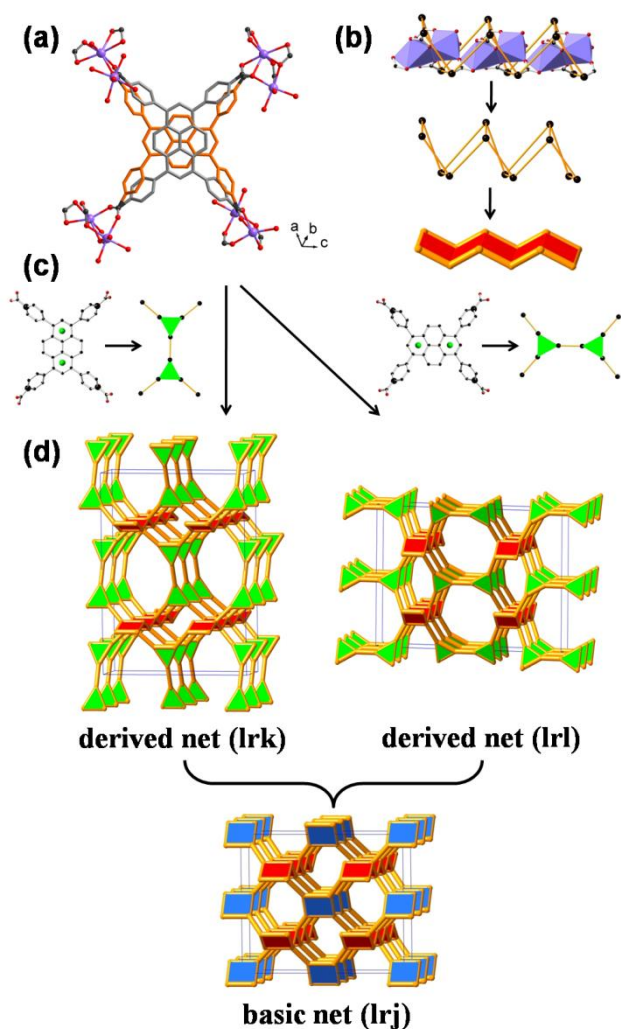


Fig. 1 Structure of ROD-8. (a) The TBAPy linker exhibiting positional disorder with two extreme positions (shown in silver and gold) in the pyrene core. (b) Deconstruction of the Cd-based rod SBU into a zigzag ladder shown in red. (c) Deconstruction of the tetratopic linker into two linked triangles (green) in the vertical or horizontal fashion corresponding to the disorder. Colour codes: Cd in indigo, O in red, C in black; H omitted. The C atoms served as points of extension are bigger than the others. (d) The underlying nets, **Ir_k** and **Ir_l** (corresponding to the two extreme positions of the linker), both derived from the basic net **Ir_j**. The blue squares in **Ir_j** can be topologically divided into the linked triangles in the derived nets. The edges of all nets are shown in gold.

Interestingly, although the positions of the carboxylate-O in TBAPy are crystallographically fixed, the voids left are sufficient for the large and flat pyrene core with four branching phenyl groups to rattle between two extreme positions of perpendicular orientations, as shown in Fig. 1a. In the refinement, these are treated as positional disorder of two parts with the refined occupancy of 0.712(3)/0.288(3),¹¹ indicated by the increased thermal ellipsoids and the residual electron density with symmetric distribution. One would have to assume that in the real crystal of ROD-8 a specific organic linker can take either position, and the overall 3D MOF experiences a type of framework disorder in the sense that the two positions can be regularly or randomly distributed in the framework.

The interest in rod MOFs¹² is linked historically back to early findings on the correlation of rod packing (also known as cylinder packing, compared with the classical sphere packing) and crystal chemistry.¹³ The proposed deconstruction method for MOFs combining both rod SBUs and polytopic linkers are illustrated by ROD-8. (i) The Cd-based rod SBU is recognized as a whole by linking the points of extension^{2b} in the rod, giving a zigzag ladder (Fig. 1b). This treatment is analogous to that of finite SBUs that are abstracted into the augmented form.¹⁴ (ii) The tetratopic organic linker is simplified as two linked three-coordinated (3-c) nodes by including the branch points (green spheres in Fig. 1c) in the tetracarboxylate, following a recent review on the topological analysis of MOFs with polytopic linkers.^{2c} (iii) For the type of MOFs combining (i) and (ii), such as ROD-8, the 3-c branch points in the linker are converted into a pair of linked triangles (Fig. 1c), in order to be consistent with the rod SBUs in which the points of extension are taken as nodes of the net. (iv) Corresponding to the two extreme positions of the ligand disorder (Fig. 1a and 1c), the vertical and horizontal alignments of the linked triangles will give rise to two different nets, namely **Ir_k** and **Ir_l**, respectively (Fig. 1d).

It is interesting to note that **Ir_k** and **Ir_l** can be considered to be derived from the basic net **Ir_j** by splitting the squares in Fig. 1d into two linked triangles in different directions. The derived net approach is a theoretical topological treatment described in a recent review.^{2c} It happens that the derived nets of **Ir_j** can describe the framework disorder of ROD-8. Note that **Ir_k** and **Ir_l** are just two simplest (highest symmetry) possibilities for the derived nets. In the actual disorder, the vertical and horizontal alignments can both occur in one framework with a regular or random distribution, but the underlying net must be always topologically derived from the basic net **Ir_j**.

As we point out^{2c} and recognized by others recently,¹⁵ the merits of taking the two linked 3-c branch points into account are (i) it gives a better reflection of the coordination geometry of the linker, and (ii) it avoids the ambiguity when two structures have the same basic net but with different derived nets. Here ROD-8 is compared with ROD-6,^{9d} a Mn MOF with the same linker, which did not show similar framework disorder and unambiguously had the net **Ir_k**. But ROD-8 can be described by two extreme ordered derived nets **Ir_k** and **Ir_l**. If considering the linker as one 4-c node, one cannot distinguish the topology between the ordered ROD-6 and disordered ROD-8 (both are **Ir_j**)—information is lost and ambiguity arises. The identification of the nets and computation of their ideal symmetry are performed through the program *Systre*,¹⁶ and the names of the nets (three-letter codes) are assigned by the database *RCSR*¹⁷ (see ESI† for detailed topological information on the **Ir_k**, **Ir_l** and **Ir_j** nets).

Powder X-ray diffraction (PXRD) measurements on the bulk material of ROD-8 showed its crystalline phase purity (Fig. S4 in ESI†). Thermogravimetric analysis (TGA) indicated that ROD-8 shows a high thermal stability up to 400 °C under nitrogen atmosphere (Fig. S3 in ESI†). ROD-8 has a high evacuation temperature at 250 °C, corresponding to the loss of solvent guests (DMF/dioxane/H₂O). Fortunately, the guest molecules can be exchanged by soaking ROD-8 in methanol, and then the

methanol can be evacuated at lower temperature (180 °C, under vacuum for 15 hours) to give the activated sample ROD-8a.

The permanent porosity of ROD-8a was confirmed by the N₂ sorption isotherm at 77 K (Fig. 2a), showing a type-I curve, with the uptake amount increasing sharply at the beginning and then reaching a plateau of 160 cm³ (STP) g⁻¹ at 1.0 atm. The BET and Langmuir surface areas are 369.3 and 572.1 m² g⁻¹ respectively, calculated from the data in the range of P/P⁰ = 0.06-0.3. At 195 K, the CO₂ and CH₄ adsorption isotherms both showed type-I curve without hysteresis, confirming the microporous character of ROD-8a. ROD-8a can store 84 cm³ (STP) g⁻¹ CH₄ (ca. 6 wt %) or 143 cm³ (STP) g⁻¹ CO₂ (ca. 28.3 wt %) at 1.0 bar.

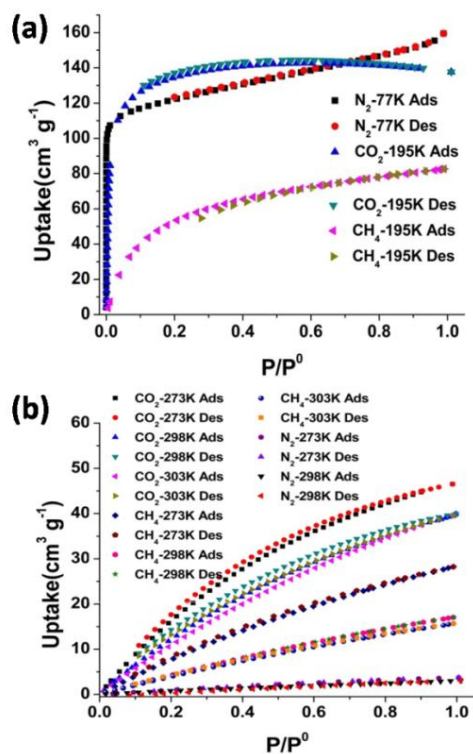


Fig. 2 Gas adsorption measurements for ROD-8a. (a) Low-temperature adsorption isotherms for N₂ at 77 K, CO₂ and CH₄ at 195 K. (b) Ambient-temperature adsorption isotherms for CO₂, CH₄ and N₂ at 273 K, 298 K and 303 K, respectively. Note: Ads—adsorption; Des—desorption.

The CO₂, CH₄ and N₂ sorption of ROD-8a was measured at ambient condition (Fig. 2b). At 298 K, the CO₂ uptake gradually increased to 40.21 cm³ (STP) g⁻¹ (ca. 7.90 wt %) at 1.0 bar. Although the amount of absorbed CO₂ at ambient temperature is moderate compared with those of best performing MOFs such as Mg-MOF-74,¹⁸ HKUST-1¹⁹ and SIFSIX-2-Cu-i,²⁰ ROD-8a can still surpass some amine-functionalized MOFs such as IRMOF-3²¹ and en-CuBTTi²² at low pressure. ROD-8a can adsorb 17.16 cm³ (STP) g⁻¹ CH₄ (ca. 0.77 wt %) at 298 K and 1 bar, higher than those of SNU-25,²³ ZIF-20²⁴ and etc. Because methane storage in MOFs is usually studied at high pressures,^{3a,g,h} it is difficult to compare ROD-8a with other MOFs such as the best performing PCN-14²⁵ and NOTT-107.²⁶ However, given the facts that (i) the nearest pyrene-pyrene distance is 4.35 Å, suited to

the CH₄ kinetic diameter of ca. 3.8 Å,^{3b} which is a preferred structural feature for enhancing methane uptake,^{3g,26} and (ii) the isosteric heat of adsorption (Fig. 3a, -Q_{st} = 16.66 to 17.93 kJ mol⁻¹ upon loading) is close to the calculated optimal value of 18.8 kJ mol⁻¹ for methane adsorbents,²⁷ the high-pressure CH₄ storage capacity of ROD-8a deserves to be further studied.

To better understand the gas adsorption preference of ROD-8a, we used IAST to predict the CO₂/N₂, CO₂/CH₄ and CH₄/N₂ selectivity at 298 K (Fig. 3b-d) and 273 K (Fig. S7 in ESI†) calculated from the single-component adsorption isotherms fitted by the dual-site Langmuir (DSL) model (see ESI† for details). Usually gas-phase adsorptive separation takes advantage of the different physical properties of the gas adsorbates (e.g. kinetic diameter [Å]: CO₂ 3.3, CH₄ 3.76, N₂ 3.64; polarizability [$\times 10^{25}/\text{cm}^3$]: CO₂ 29.11, CH₄ 25.93, N₂ 17.40; quadrupole moment [$\times 10^{26}/\text{esu}\cdot\text{cm}^2$]: CO₂ 4.30, CH₄ 0, N₂ 1.52),^{3b} especially the much larger quadrupole moment of CO₂ that can interact with the open metal sites or polar organic groups in the pore surface of functionalized MOFs,^{3d} facilitating CO₂/N₂ and CO₂/CH₄ selectivity.^{3c,7,28} Most recently attention has been paid to CH₄/N₂ separation which is more difficult because of the similar physical parameters for N₂ and CH₄.²⁹

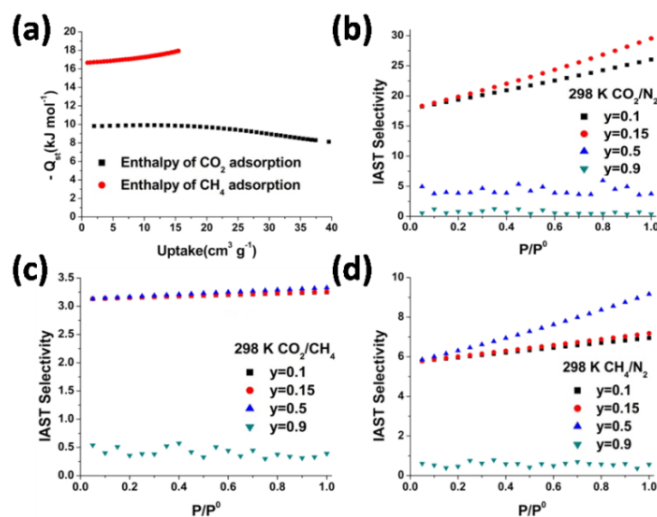


Fig. 3 Selective gas adsorption analysis for ROD-8a, showing (a) isosteric adsorption enthalpy (-Q_{st}) plot for CO₂ and CH₄ adsorption calculated using Clausius-Clapeyron equation at ambient temperature, and IAST predicted (b) CO₂/N₂, (c) CO₂/CH₄ and (d) CH₄/N₂ selectivity at various gas mixture ratios (y) calculated from DSL fitting at 298 K.

The very low -Q_{st} of CO₂ (Fig. 3a) indicates the lack of classical interacting site in ROD-8a. The IAST predictions show a CO₂/N₂ (85:15 mixture) selectivity of ca. 29 at 298 K and 1 bar (Fig. 3b), but no significant preference of CO₂ over CH₄ is observed (Fig. 3c). Interestingly, ROD-8a exhibits selective adsorption of CH₄ over N₂ (ca. 9 at 50:50 ratio) at 298 K and 1 bar (Fig. 3d, higher at 273 K; ca. 17). Compared with N₂, CH₄ is even non-dipolar and non-quadrupolar, and with higher critical temperature (T_c = 191 K; N₂ 126 K). These results are consistent with the above speculation, based on structural and -Q_{st} analysis, on the potential CH₄ storage capacity of ROD-8a.

In summary, a new Cd-based rod MOF, ROD-8, has been synthesized and studied. Crystallographic analysis reveals there is positional disorder in the tetratopic pyrene-core linker. The deconstruction method for MOFs with both rod SBUs and polytopic linker is illustrated by the topological analysis of ROD-8. The underlying nets, **lrk** or **lrl**, both derived from **lrj**, can describe two extreme ordered situations of the framework of ROD-8. Meanwhile, the structural feature, suitable adsorption enthalpy and IAST selectivity of the activated ROD-8a indicate its potential for further high-pressure CH₄ adsorption study.

D.L. and X.P.Z. is financially supported by the National Basic Research Program of China (973 Program, 2012CB821706 and 2013CB834803), the National Natural Science Foundation of China (91222202, 21171114, 21101103 and 21371113), and the Natural Science Foundation of Guangdong Province (S201140004334). S.W.N. thanks the funding of the Ministry of Higher Education of Malaysia (Grant No. UM.C/HIR-MOHE/SC/03). M.O'K. is supported by the U.S. National Science Foundation (grant DMR 1104798).

Notes and references

^a Department of Chemistry and Research Institute for Biomedical and Advanced Materials, Shantou University, Guangdong 515063, P.R. China. E-mail: zhouxp@stu.edu.cn (X.P.Z.); dli@stu.edu.cn (D.L.)

^b Department of Chemistry, University of Malaya, 50603 Kuala Lumpur, Malaysia; Chemistry Department, Faculty of Science, King Abdulaziz University, PO Box 80203 Jeddah, Saudi Arabia

^c Department of Chemistry and Biochemistry, Arizona State University, Tempe, Arizona 85287, United States. E-mail: mokeeffe@asu.edu (M.O'K.)

† Electronic Supplementary Information (ESI) available: Experimental details, crystal structure description, topological information, additional characterization, gas adsorption measurements and analysis. For ESI and crystallographic data in CIF or other electronic format see DOI: 10.1039/c000000x/

‡ Crystal data for ROD-8: C₄₉H₃₇Cd₂NO₁₂, *M_r* = 1012.54, monoclinic, space group *P2₁/c*, *a* = 7.1510(1), *b* = 24.8988(4), *c* = 28.6097(4) Å, β = 93.406(1)°, *V* = 5085.00(13) Å³, *Z* = 4, ρ_{calcd} = 1.323 g·cm⁻³, no. of reflns/unique = 14688 / 8079, *R_{int}* = 0.0481, *R₁* [*I* ≥ 2σ(*I*)] = 0.0523, *wR₂* [*I* ≥ 2σ(*I*)] = 0.1249, GOF = 1.060. CCDC 984649.

- (a) S. R. Batten, N. R. Champness, X.-M. Chen, J. Garcia-Martinez, S. Kitagawa, L. Öhrström, M. O'Keeffe, M. P. Suh and J. Reedijk, *Pure Appl. Chem.*, 2013, **85**, 1715; (b) S. R. Batten, N. R. Champness, X.-M. Chen, J. Garcia-Martinez, S. Kitagawa, L. Öhrström, M. O'Keeffe, M. P. Suh and J. Reedijk, *CrystEngComm*, 2012, **14**, 3001.
- (a) H. Furukawa, K. E. Cordova, M. O'Keeffe and O. M. Yaghi, *Science*, 2013, **341**, 1230444; (b) M. O'Keeffe and O. M. Yaghi, *Chem. Rev.*, 2012, **112**, 675; (c) M. Li, D. Li, M. O'Keeffe and O. M. Yaghi, *Chem. Rev.*, 2014, **114**, 1343; (d) E. V. Alexandrov, V. A. Blatov, A. V. Kochetkov and D. M. Proserpio, *CrystEngComm*, 2011, **13**, 3947.
- (a) R. B. Getman, Y.-S. Bae, C. E. Wilmer and R. Q. Snurr, *Chem. Rev.*, 2012, **112**, 703; (b) J.-R. Li, R. J. Kuppler and H.-C. Zhou, *Chem. Soc. Rev.*, 2009, **38**, 1477; (c) J.-R. Li, Y. Ma, M. C. McCarthy, J. Sculley, J. Yu, H.-K. Jeong, P. B. Balbuena and H.-C. Zhou, *Coord. Chem. Rev.*, 2011, **255**, 1791; (d) K. Sumida, D. L. Rogow, J. A. Mason, T. M. McDonald, E. D. Bloch, Z. R. Herm, T.-H. Bae and J. R. Long, *Chem. Rev.*, 2012, **112**, 724; (e) J.-R. Li, J. Sculley and H.-C. Zhou, *Chem. Rev.*, 2012, **112**, 869; (f) M. P. Suh, H. J. Park, T. K. Prasad and D.-W. Lim, *Chem. Rev.*, 2012, **112**, 782; (g) T. A. Makal, J.-R. Li, W. Lu and H.-C. Zhou, *Chem. Soc. Rev.*, 2012, **41**, 7761; (h) Y. He, W. Zhou, R. Krishna and B. Chen, *Chem. Commun.*, 2012, **48**, 11813.
- A. Corma, H. García and F. X. Llabrés i Xamena, *Chem. Rev.*, 2010, **110**, 4606.
- L. E. Kreno, K. Leong, O. K. Farha, M. Allendorf, R. P. Van Duyne and J. T. Hupp, *Chem. Rev.*, 2012, **112**, 1105.
- Y. Yan, S. Yang, A. J. Blake and M. Schröder, *Acc. Chem. Res.*, 2014, **47**, 296.
- G. Férey, C. Serre, T. Devic, G. Maurin, H. Jobic, P. L. Llewellyn, G. De Weireld, A. Vimont, M. Daturi and J.-S. Chang, *Chem. Soc. Rev.*, 2011, **40**, 550.
- A. L. Myers and J. M. Prausnitz, *AIChE J.*, 1965, **11**, 121.
- (a) Z. Yan, M. Li, H.-L. Gao, X.-C. Huang and D. Li, *Chem. Commun.*, 2012, **48**, 3960; (b) J. Xiao, Y. Wu, M. Li, B.-Y. Liu, X.-C. Huang and D. Li, *Chem. Eur. J.*, 2013, **19**, 1891; (c) H.-L. Zhou, M. Li, D. Li, J.-P. Zhang and X.-M. Chen, *Sci. China Chem.*, 2014, **57**, 365; (d) R.-J. Li, M. Li, X.-P. Zhou, D. Li and M. O'Keeffe, *Chem. Commun.*, 2014, **50**, DOI: 10.1039/C3CC49684H.
- (a) K. C. Stylianou, R. Heck, S. Y. Chong, J. Bacsá, J. T. A. Jones, Y. Z. Khimyak, D. Bradshaw and M. J. Rosseinsky, *J. Am. Chem. Soc.*, 2010, **132**, 4119; (b) K. C. Stylianou, J. Rabone, S. Y. Chong, R. Heck, J. Armstrong, P. V. Wiper, K. E. Jelfs, S. Zlatogorsky, J. Bacsá, A. G. McLennan, C. P. Ireland, Y. Z. Khimyak, K. M. Thomas, D. Bradshaw and M. J. Rosseinsky, *J. Am. Chem. Soc.*, 2012, **134**, 20466; (c) J. E. Mondloch, W. Bury, D. Fairen-Jimenez, S. Kwon, E. J. DeMarco, M. H. Weston, A. A. Sarjeant, S. T. Nguyen, P. C. Stair, R. Q. Snurr, O. K. Farha and J. T. Hupp, *J. Am. Chem. Soc.*, 2013, **135**, 10294; (d) P. Deria, J. E. Mondloch, E. Tylianakis, P. Ghosh, W. Burry, R. Q. Snurr, J. T. Hupp and O. K. Farha, *J. Am. Chem. Soc.*, 2013, **135**, 16801.
- (a) S. W. Ng, *Chinese J. Struct. Chem.*, 2005, **24**, 1425; (b) X.-P. Zhou, M. Li, J. Liu and D. Li, *J. Am. Chem. Soc.*, 2012, **134**, 67; (c) A. B. Cairns and A. L. Goodwin, *Chem. Soc. Rev.*, 2013, **42**, 4811.
- N. L. Rosi, J. Kim, M. Eddaoudi, B. Chen, M. O'Keeffe and O. M. Yaghi, *J. Am. Chem. Soc.*, 2005, **127**, 1504.
- (a) S. Andersson and M. O'Keeffe, *Nature*, 1977, **267**, 605; (b) M. O'Keeffe and S. Andersson, *Acta Cryst. A*, 1977, **33**, 914.
- D. J. Tranchemontagne, J. L. Mendoza-Cortés, M. O'Keeffe and O. M. Yaghi, *Chem. Soc. Rev.*, 2009, **38**, 1257.
- D. Frahm, F. Hoffmann and M. Fröba, *Cryst. Growth Des.*, 2014, **14**, DOI: 10.1021/cg4018536.
- O. Delgado-Friedrichs and M. O'Keeffe, *Acta Crystal. A*, 2003, **59**, 351. *Systre* is available at <http://www.gavrog.org/>
- M. O'Keeffe, M. A. Peskov, S. J. Ramsden and O. M. Yaghi, *Acc. Chem. Res.*, 2008, **41**, 1782. *RCSR* (Reticular Chemistry Structure Resource) is available at <http://rcsr.anu.edu.au/>
- (a) J. A. Mason, K. Sumida, Z. R. Herm, R. Krishna and J. R. Long, *Energy Environ. Sci.*, 2011, **4**, 3030; (b) D. Britt, H. Furukawa, B. Wang, T. G. Glover and O. M. Yaghi, *Proc. Natl. Acad. Sci. U.S.A.*, 2009, **106**, 20637.
- A. O. z. r. Yazaydin, A. I. Benin, S. A. Faheem, P. Jakubczak, J. J. Low, R. R. Willis and R. Q. Snurr, *Chem. Mater.*, 2009, **21**, 1425.
- P. Nugent, Y. Belmabkhout, S. D. Burd, A. J. Cairns, R. Luebke, K. Forrest, T. Pham, S. Ma, B. Space, L. Wojtas, M. Eddaoudi and M. J. Zaworotko, *Nature*, 2013, **495**, 80.

- 21 A. R. Millward and O. M. Yaghi, *J. Am. Chem. Soc.*, 2005, **127**, 17998.
- 22 A. Demessence, D. M. D'Alessandro, M. L. Foo and J. R. Long, *J. Am. Chem. Soc.*, 2009, **131**, 8784.
- 23 Y. E. Cheon, J. Park and M. P. Suh, *Chem. Commun.*, 2009, 5436.
- 24 H. Hayashi, A. P. Côté, H. Furukawa, M. O'Keeffe and O. M. Yaghi, *Nat. Mater.*, 2007, **6**, 501.
- 25 S. Ma, D. Sun, J. M. Simmons, C. D. Collier, D. Yuan and H.-C. Zhou, *J. Am. Chem. Soc.*, 2007, **130**, 1012.
- 26 C. E. Wilmer, M. Leaf, C. Y. Lee, O. K. Farha, B. G. Hauser, J. T. Hupp and R. Q. Snurr, *Nat. Chem.*, 2012, **4**, 83.
- 27 S. K. Bhatia and A. L. Myers, *Langmuir*, 2006, **22**, 1688.
- 28 J. Duan, M. Higuchi, S. Horike, M. L. Foo, K. P. Rao, Y. Inubushi, T. Fukushima and S. Kitagawa, *Adv. Funct. Mater.*, 2013, **23**, 3525.
- 29 K. Lee, W. C. Isley III, A. L. Dzubak, P. Verma, S. J. Stoneburner, L.-C. Lin, J. D. Howe, E. D. Bloch, D. A. Reed, M. R. Hudson, C. M. Brown, J. R. Long, J. B. Neaton, B. Smit, C. J. Cramer, D. G. Truhlar and L. Gagliardi, *J. Am. Chem. Soc.*, 2014, **136**, 698.

For Graphic Abstract: